# Results from a Series of Tethered Rocket Experiments

S. Sasaki,* K.I. Oyama,† N. Kawashima,‡ Y. Watanabe,§ and T. Obayashi¶
*Institute of Space and Astronautical Science, Tokyo, Japan*
W.J. Raitt** and A.B. White††
*Utah State University, Logan, Utah*
P.M. Banks‡‡ and P.R. Williamson§§
*Stanford University, Stanford, California*
W.F. Sharp¶¶
*University of Michigan, Ann Arbor, Michigan*
T. Yokota***
*Ehime University, Ehime, Japan*
and
K. Hirao†††
*Tokai University, Kanagawa, Japan*

**Tethered rocket experiments have been carried out three times during a U.S.-Japan joint space program in progress since 1980. The results provide a preliminary test for the U.S.-Italy Tethered Satellite System-1 experiments scheduled for flight with the Space Shuttle in the early 1990s. The goal of the rocket program has been to perform a new type of active experiment by ejecting an electron beam from the tethered mother-daughter payload system. Several important results have been obtained in the series of experiments. In the third rocket flight, the conductive tether wire was deployed to 418 m, which was the first time the wire length exceeded 100 m in the sounding rocket experiments. The vehicle charging due to dc beam emission up to 80 mA in the altitude range from 150 to 200 km was repeatedly measured by both Langmuir and floating probes, and was found to be usually less than 10 V. In addition, during the 80-mA emission, clear evidence for the ignition of a beam-plasma discharge was obtained by the plasma probe, photometers, and wave receivers. In the tether deployment experiment, it was found that the tether wire acted as an antenna and its antenna impedance decreased with the extension of the wire both in high-frequency and very low-frequency bands. Finally, substantial rocket charging (to greater than 100 V) was observed during periods of electron beam very low-frequency pulsing.**

## I. Introduction

A TETHERED payload system in which two separate payloads in space are connected with an insulated conductive wire has been proposed to conduct a new type of active experiment combined with electron beam emission (Shuttle Electrodynamic Tether System, SETS).[1] By applying a high voltage between the two payloads connected with a conductive wire, the response of ionospheric plasma to large potential differences between the collector and the plasma can be studied. In the passive case, the current between the two payloads will be limited by the collection of the ion current at the negatively biased payload because the ion saturation current is much less than the electron saturation current in the ionosopheric plasma. With electron beam emission at one end, the tether current can be controlled. By modulating the beam current, low-frequency radio waves with long wavelength, such as whistler and Alfvén modes, will be excited in a well-controlled manner.

The tethered payload system is very useful as a diagnostic of the electron beam experiment itself. The electron beam emission generates a large-scale modification of the plasma parameters up to 100 m or more surrounding the vehicle,[2] which has resulted in difficulty in understanding the total process of beam-plasma interaction by measurements from the same payload. Using a daughter payload installed with diagnostics separating from the mother payload which emits an electron beam, the surrounding plasma condition can be measured in a large scale. The potential of the mother payload can easily be determined without ambiguity by measuring the potential difference from the daughter payload when it reaches outside of the turbulent plasma region. The same idea—to use a tethered satellite as a diagnostic system—has recently been proposed in another active experiment to study Alfvén's critical ionization velocity by Xenon release from the Space Shuttle.[3]

Tether systems will be used in the future as a new means of diagnosis in the lower ionosphere, where a satellite cannot keep its orbit due to the strong drag force. The lower ionosphere—below 200 km, especially around 100 km—is perturbed by many active plasma phenomena, which are

Received Nov. 5, 1985; revision received Aug. 4, 1986. 

*Research Associate, Division of Planetary Science.
§Engineer, Division of Space Plasma.
¶Director, Space Plasma Division.
**Professor, Department of Physics.
††Senior Research Project Engineer, Center for Space Engineering.
‡‡Professor, STAR Laboratory, Department of Electrical Engineering. Member AIAA.
§§Senior Research Associate, STAR Laboratory, Department of Electrical Engineering. Member AIAA.
¶¶Research Scientist, Space Physics Research Lab.
***Associate Professor, Faculty of General Education.
†††Professor, School of Engineering.

geophysically interesting related to the generation of neutral wind and ionospheric currents. The idea to use the Space Shuttle with a tethered subsatellite extended down to the lower ionosphere from the orbital height (~250 km) has been proposed and investigated as a powerful and feasible system to research the lower ionosphere.[4-6] The vertical long wire will stabilize the dynamics of the tethered subsatellite by gravity gradient forces. Using a multiple-tethered subsatellite system, the vertical structure of the lower ionosphere can be instantaneously measured.

In this paper, the results of three tethered rocket experiments conducted as part of a U.S.-Japan joint program under way since 1980 (Tethered Payload Experiment; TPE series) are reported. The major purpose of the experiments has been to obtain technical and scientific data supporting the future electrodynamic tethered subsatellite experiments by the Space Shuttle, currently scheduled for 1990 as part of the Tethered Satellite System-1 Mission. The first two experiments reported here were done under collaboration of the Institute of Space and Astronautical Science (ISAS) and the Center for Atmospheric and Space Science of Utah State University (USU) using Japanese sounding rockets K-9M-69 and S-520-2.[7] In these experiments, a tether wire was deployed to lengths of 38 and 65 m, respectively, although total deployments of 400 m were planned. In the last experiment, under collaboration of USU, ISAS, Stanford University, and the University of Michigan, using the NASA Black Brant V rocket, the wire was successfully deployed to 418 m, as planned. In all of these rocket flights, an electron beam up to 1 kV and 80 mA was injected before mother-daughter separation. The rocket charging potential has been measured repeatedly in these experiments by very similar instruments, and reproducible data have been obtained. In the third flight, the beam was injected in a well-controlled configuration parallel to the magnetic field, and observations of a space beam-plasma interaction were obtained, just as in laboratory electron beam experiments.

Unfortunately, the active electron beam experiments after payload separation were not successful, due to failures of the payload battery pack supplying high-voltage power in the three flights. However, passive plasma observations were continued correctly after the separations. The dynamics of tether wire were observed by a charge-coupled device (CCD) TV camera in the second experiment. A strong effect of the wire extension on the background wave measurements was found unexpectedly in the last experiment.

## II. Experiment

The payload instruments are basically the same in the three experiments. The onboard instruments in the series of experiments are listed in Table 1. The tether deployment system was installed on the mother rocket in the first two experiments, and on the daughter rocket in the last experiment. Figure 1 shows the configuration of the payloads in the last experiment.

The mother payload was composed of an electron gun, a floating/Langmuir probe array, a thermal electron energy detector, photometers, cameras, an electrostatic electron energy analyzer, a charge probe, and a tether voltage/current monitor. The electron gun (Fast Pulse Electron Gun; FPEG) generated a narrow electron beam of 1 kV, 80 mA (peak current) in dc and multipulse modes (2, 8, 32, and 256 $\mu$s). The floating/Langmuir probe array (PLP) consisted of four cylindrical probes installed on a rod every 25 cm, which was deployed after despin. The thermal electron energy detector (TED) was deployed to a distance of 1 m from the rocket skin. The sensor was protected by a glass envelope until deployment to avoid electrode contamination. Two 35-mm cameras with high-sensitivity color film (ASA 800) were also installed. One was operated synchronized with the beam firings to observe the beam trajectory. Another was synchronized with flashing of a strobe light to illuminate the reflective tape attached to the daughter rocket. Two photometers filtered at 3914 Å were used to detect the light emission from the interaction of the electron beam with the atmosphere and from the charge sheath around the rocket surface skin. The charge probe, a dc/dc converter to apply a high voltage up to 500 V between the two payloads, and the tether voltage/current monitor were assembled in one unit (Mother Charge Probe). A wire tension monitor and a mechanism to cut the wire at the re-entry to the atmosphere were installed at the end of the tether wire. The operation of the FPEG, cameras, photometers, MCP, and fast data handling unit were controlled by a microprocessor.

The daughter payload consisted of the Tether Deployment System (TDS), high-frequency (hf)/very low-frequency(vlf) wave receivers, and a charge probe (DCP). The TDS contained 418 m of wire and a deployment monitoring system with 0.1 m resolution. The wire was stainless steel, 0.66 mm in diameter, and coated with teflon. Two sets of 2.4-m-dipole antennas (tip-tip) were used for the wave detection. High-frequency wave signals from 0.2 to 10 MHz were analyzed as a frequency spectrum every 250 ms. Very low-frequency wave signals in a broad band from 0.4 to 30 kHz were directly transmitted to ground via an S-band telemetry link.

K-9M-69 was launched at 12:00 Japanese Standard Time (JST) on January 16, 1980, with an elevation angle of 77 deg from Kagoshima Space Center at Uchinoura. It reached a maximum altitude of 328 km at 292 s after launch. The electron beam of 0.5 kV, 22 mA and 1 kV, 30 mA was injected from 90 to 106 s (150-180 km). The mother-daughter rocket was separated at 106 s (180 km) with a velocity of 0.5 m/s. The wire was deployed to a distance of 38 m.

The second flight, S-520-2, was launched at 16:00 JST on January 29, 1981, with an elevation angle of 80 deg from Kagoshima Space Center. It reached a maximum altitude of 322 km at 337 s. The beam of 1 kV, 30 mA was injected at around a height of 200 km. The rocket was separated at 134 s (220 km) with a velocity of 1 m/s. The tether wire was deployed with an extension of 65 m.

The third experiment was carried out by Black Brant V, launched at 00:00 Mountain Daylight Time on August 8, 1983, from White Sands Missile Range, NM. It reached a maximum altitude of 218 km. An electron beam of up to 1 kV, 80 mA was injected parallel to the magnetic field from 117 s to 144 s (142-169 km). The rocket was separated at 153 s (175 km) with a velocity of 1.5 m/s. The tether wire was deployed to a length of 418 m during 283 s.

## III. Experimental Results

### A. Tether Wire Deployment and Dynamics

The tether wire started to deploy at the mother-daughter separation by a multiple spring system. The separation speed

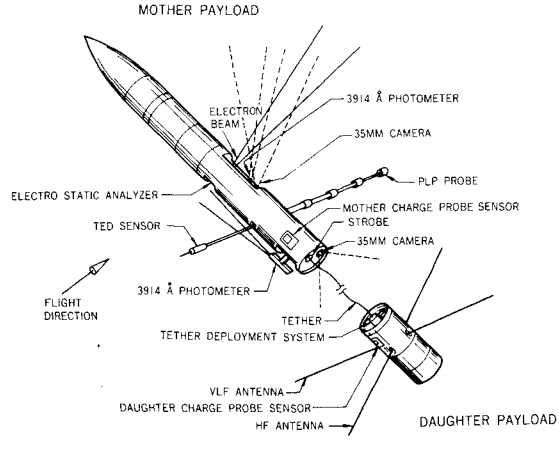


**Fig. 1 Payload configuration in the third experiment.**

was set at 0.5, 1.0, and 1.5 m/s in the first, second, and third experiments, respectively. Figure 2 shows the deployment of the tether wire plotted against time in the three experiments. In the first two experiments, the deployment speed gradually decreased with time and finally stopped abruptly at 38 and 65 m, respectively, due to a frictional force in the tether deployment system. The maximum frictional force was estimated to be greater than 2 kg-W. In the last experiment, an improved deployment system with less friction was flown, and a Reaction Control System (RCS) on board the daughter rocket was operated every 40 s to compensate for the friction. At the bottom, the thrustering of RCS is designated. No clear relation is seen between the thrustering and extension velocity, which means that the wire slackened after it went out from the deployment system and the force generated by the thrustering did not propagate to the deployment system directly. This situation has been actually observed by a solid-state TV camera[8] in the second experiment, in which the wire was observed twisting due to its springiness (Fig. 3). This occurs naturally when the spring force is larger than the frictional force at the deployment system or the drag force. The gravitational force generated by the gravity gradient is negligible for the present case. In the third experiment, there was a clear deceleration of the deployment speed by 30% at around 140 s. At that moment, an abnormally large tension was detected for 0.25 s by the tension monitor. This was caused by an increase of frictional force beyond 1 kg-W pulsively generated at the deployment system. The slack of the wire at this moment is calculated as about 1%. The increase of the deployment speed at the last phase around 270 s is explained by the drag effect below the altitude of 100 km. The wire snapped at 283 s, when it extended out just before the wire cutter was activated. The wire snapped again near the daughter payload at the altitude of 47 km due to drag.

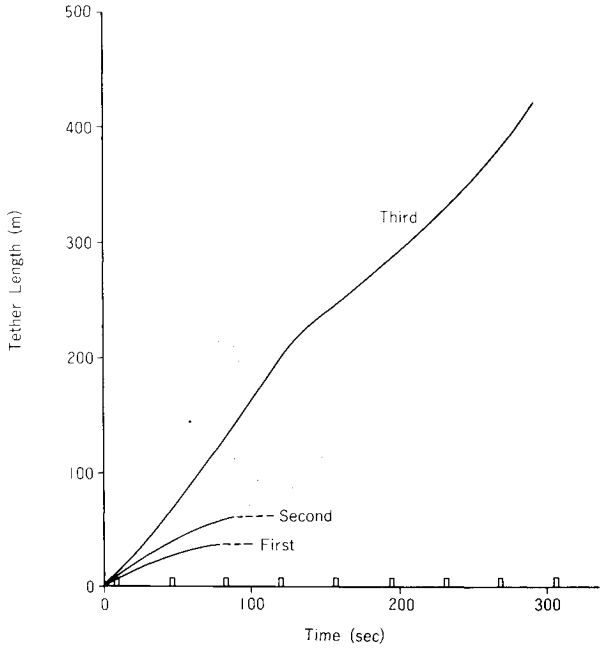


**Fig. 2 Deployment of tether wire in the TPE series.**

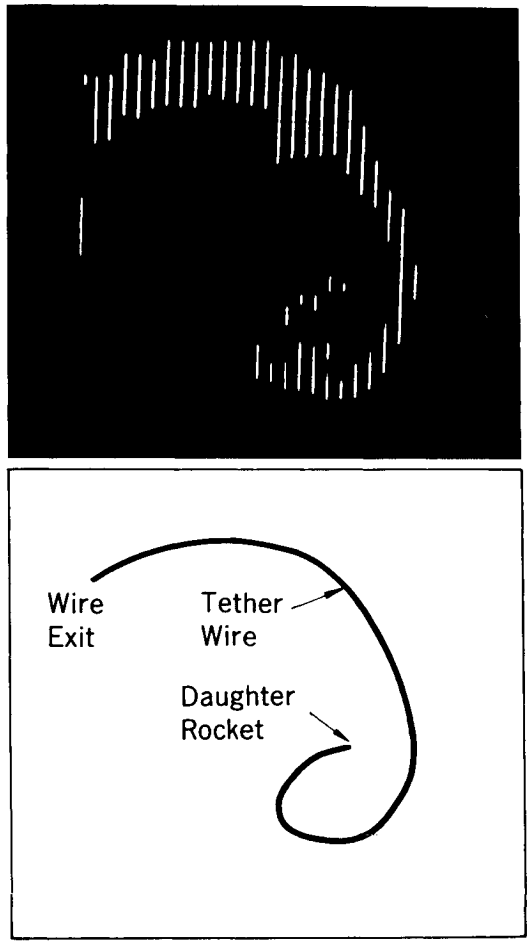


**Fig. 3 Tether wire observed by a TV camera (32×32 elements) onboard mother rocket in the second experiment.**

**Table 1 Payload instruments in tethered payload experiment (TPE) series**

| | TPE-1 | TPE-2 | TPE-3 |
|---|---|---|---|
| Rocket | K-9M-69 | S-520-2 | Black Brant V |
| Launch date | Jan. 16, 1980 | Jan. 29, 1981 | Aug. 8, 1983 |
| Launch site | Kagoshima Space Center | Kagoshima Space Center | White Sands Missile Range |
| Mother payload | Electron gun (1 kV, 30 mA max) | Electron gun (1 kV, 30 mA) | Electron gun (1 kV, 80 mA max) |
| | Langmuir/floating probe | Return current monitor | Langmuir/floating probe array |
| | Charge probe | Charge probe | Charge probe |
| | Electron energy analyzer | Electron energy analyzer | Electrostatic analyzer |
| | Optical detector array | CCD camera | Still camera (2) |
| | Tether deployment system | Tether deployment system | Photometer (2) |
| | Flashing lamp | Tether V/I monitor | Flashing lamp |
| | Tether V/I monitor | | Tether V/I monitor |
| Daughter payload | vlf Receiver | vlf Receiver | vlf Receiver |
| | hf Receiver | hf Receiver | hf Receiver |
| | Langmuir/floating probe | Langmuir/floating probe array | Tether deployment system |
| | Charge probe | Charge probe | Charge probe |
| | Impendance probe | | |

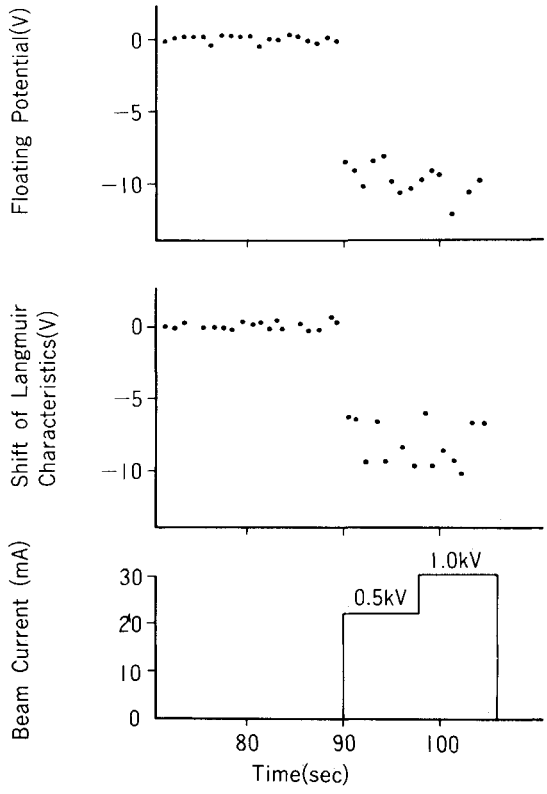


**Fig. 4 Rocket potential measured by a floating probe and a Langmuir probe in the first experiment.**

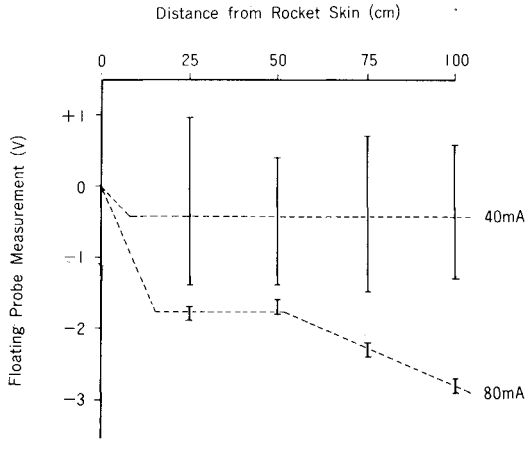


**Fig. 5 Rocket potential measured by a floating probe array in the third experiment.**

### B. Potential and Plasma Measurement During Beam Emission

Two sets of floating probes and Langmuir probes close to the rocket skin were used in the first experiment. In the second and third experiments, a floating probe array composed of four probes was extended up to 1–1.2 m from the rocket skin. This array was also used as a Langmuir probe by time-sharing of the bias, which was swept from -10 to 10 V in 125 ms. The measurement of the floating probe corresponds to the vehicle potential with respect to the floating potential of the surrounding plasma when the impedance for voltage detection in the electronics is larger than the probe impedance to the surrounding medium. If the probe is located inside the electron sheath and if plasma is produced there, the measurement is lower than the vehicle potential. On the other hand, the vehicle potential can be derived more accurately from the shift of the onset bias of the electron current in the Langmuir probe characteristics.

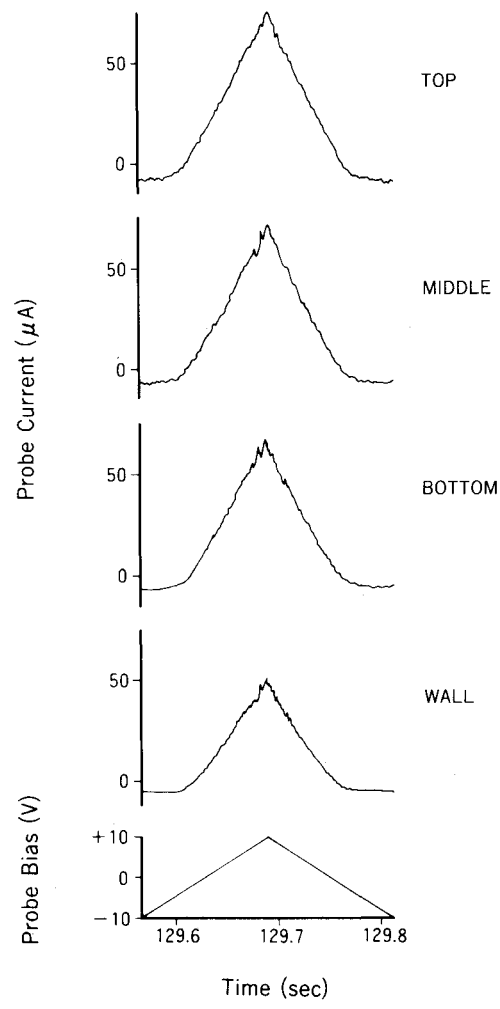


**Fig. 6 Langmuir characteristics obtained by the four probes during 1-kV, 80-mA beam emission in the third experiment.**

Figure 4 shows the measurements of the floating probe and vehicle potential derived from the shift of the Langmuir characteristics in the first experiment (0.5 kV, 22 mA; 1 kV, 30 mA; 150–180 km in altitude). The measurements of the floating probe (8.6–12.3 V) modulated by spin motion approximately coincide with the potential rise (6-10.2 V) derived from the shift of the onset bias of the electron current in the Langmuir characteristics. No clear difference is seen between the two beam energies (0.5 and 1 kV). In the second experiment (1 kV, 30 mA; 200 km in altitude), the vehicle potential was estimated as 5–10 V.[9]

In the third experiment (140–170 km in altitude), the rocket was despun before the beam emission and was controlled so that the beam was injected parallel to the magnetic field. The beam current was set at 5, 10, 40, and 80 mA. Figure 5 shows the measurements of floating probes for the beam current at 40 and 80 mA. The measurement is 1.8–2.8 V for the 80-mA beam. In the 5- and 80-mA cases, the potential rise is also derived from the shift of Langmuir characteristics as 0.1–0.8 V and 1.0–2.4 V, respectively. The approximate coincidence of the potential measurements by the floating probe and by the shift of Langmuir characteristics indicates that the extended probe was located outside the plasma sheath, and the rocket potential could be measured properly by the probe although the surrounding plasma was disturbed more or less by a wave-particle interaction, as discussed later. Table 2 summarizes the potential rise due to the stationary beam injection measured in the three experiments.

It is concluded that the potential rise is commonly less than 10 V for the beam up to 80 mA in the altitude range from 150

**Table 2 Summary of potential measurements during the beam injection in the tethered payload experiment (TPE) series**

| | TPE-1 | | TPE-2 | TPE-3 | | | |
|---|---|---|---|---|---|---|---|
| Local time | 12:00, Jan. 16 | | 16:00, Jan. 29 | 00:00, Aug. 8 | | | |
| Altitude, km | 150~180 | | 200 | 140~170 | | | |
| Beam energy, kV | 0.5 | 1 | 1 | 1 | 1 | 1 | 1 |
| Beam current, mA | 22 | 30 | 30 | 5 | 10 | 40 | 80 |
| Potential rise, V | 6.3-9.3 | 6.0-10.2 | 5-10 | 0.1-0.8 | ≤1 | ≤1 | 1.0-2.4 |

to 200 km, regardless of the difference of local time and payload size. Since the electron current density from the ionospheric plasma is generally less than 1 mA/m$^2$ at these altitudes and the conductive surface area of the rocket is less than 2 m$^2$, such low charging effects cannot be explained by conventional single probe theories[10-12]; plasma production by the beam injection must be an important process in the electrical neutralization.

Figure 6 shows the Langmuir characteristics during the beam injection (80 mA) in the third experiment. It shows that the plasma density measured during the beam emission increased with the distance from the rocket. The plasma density derived from the Langmuir current of the top probe (1 m from the wall) reaches approximately $10^7$/cm$^3$ ($T_e \sim 1000$ K is assumed), while the background density is measured as $10^4$/cm$^3$. The plasma density inside the beam produced by electron beam-ionospheric gas impact ionization is calculated as $5\times10^4$/cm$^3$ for the beam current of 80 mA at the altitude of 150 km. (A neutral gas density of $6\times10^{10}$/cm$^3$, a beam radius of 10 cm, an ionization cross section of $9\times10^{-17}$ cm$^2$, and a radial plasma diffusion speed of 2000 m/s were used.) From this, it can be seen that a large plasma density detected outside the beam cannot be explained by a simple primary electron beam-neutral gas impact ionization process, but that we must consider plasma production by additional suprathermal electrons generated by a beam-plasma collective interaction.

In the third experiment, the gun was also operated in a pulsed mode with a square wave at 80 mA. The on-off time was either 256, 32, 8, or 2$\mu$s (duty ratio 50%). In contrast to the dc beam injection, the potential rise was prominently large in the pulsating beam injection (Fig. 7). The temporal change during 256- and 8-$\mu$s injection was due to malfunctions of the electron gun and is not significant. The measurement of the floating potential at the top probe exceeded 100 V constantly when the pulsing was slower than 2 $\mu$s, while it changed with time from high to low for 2-$\mu$s pulsing. The other inner probe measurements had qualitatively the same features as the top probe measurement. The fact that substantial rocket charging occurred with low-frequency (256 $\mu$s) square-wave pulsing is in conflict with the dc pulsing results. In addition, the time-dependent reduction of rocket potential for high-frequency (2 $\mu$s) pulsing provides another seemingly contradictory result.

### C. Optical Measurements During Beam Emission

The third experiment was carried out in nighttime during new moon to make optical observations using two photometers filtered at 3914 Å and a still camera. Photometer A, installed on the same side of the rocket as the electron gun, looked at the beam path, and photometer B, installed on the opposite side to the gun, detected the light emission in the sheath near the rocket skin. Figure 8 shows the light intensity detected by the two photometers and the beam appearance observed by the still camera.

The aurora line at 3914 Å from the beam is produced by the reaction process

$$N_2 + e \rightarrow N_2^+ + 2e + h\nu$$

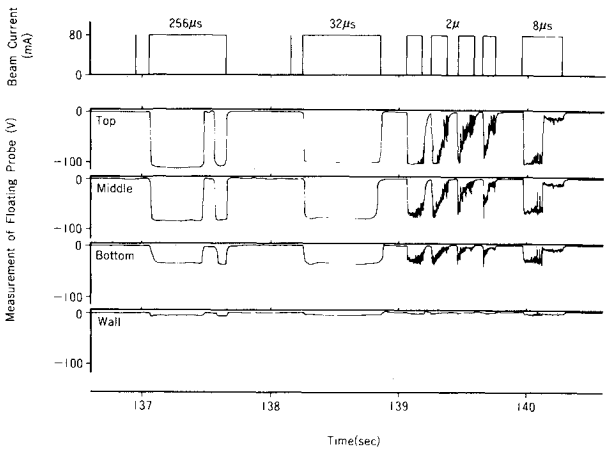


**Fig. 7 Floating probe measurements in the pulsating beam injection in the third experiment.**

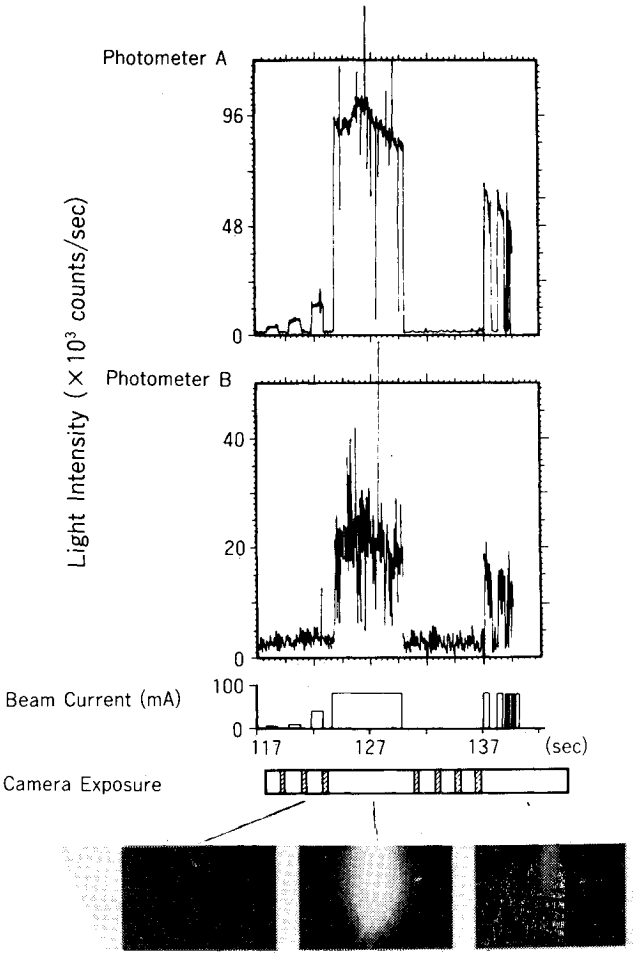


**Fig. 8 Light intensity observed by the two photometers filtered at 3914 Å. The still camera looks up to the beam.**

The photon production rate by the beam-gas impact excitation is expressed as $n_n \sigma J_b/e$, where $n_n$ is $N_2$ density, $\sigma$ the 3914 Å production cross section, $J_b$ the beam current density, and $e$ the electronic charge. The photon production rate per unit volume is proportional to the beam current density and $N_2$ density. The light intensity for the first two steps (5 and 10 mA) detected by photometer A increased linearly with the beam current. The light intensity for the third step did not increase as much as the increment of the beam current from the second step, which was possibly caused by the reduction of the beam current density due to its space charge. The light intensity increased remarkably by almost one order of magnitude when the beam current increased from 40 to 80 mA. This cannot be explained by the beam-background gas impact excitation alone. The strong excitation of the visible emission at 80 mA was also observed by the still camera. No beam trajectory was detected for the 40-mA beam (exposure time of 1.4 s), however, a clear image was taken for 80 mA (exposure time of 7.8 s). Taking the exposure time into consideration, the difference of the luminosity of the beam also cannot be explained by the increase of beam current. The abrupt change of the luminosity with increasing beam current has been observed in the laboratory experiments of the Beam Plasma Discharge (BPD). In an experiment in the large vacuum facility at Johnson Space Center,[13] four states of the light emission from the beam and ambient gas were observed depending on the beam current at the low pressure below $4 \times 10^{-6}$ Torr; collisional excitation by the primary beam, weak glow surrounding the beam, beam plasma discharge, and second-stage beam plasma discharge. In these experiments, the light emission increased approximately linearly with increases in the beam current, and a jump in luminosity appeared as the beam plasma discharge was ignited. The large amount of plasma production described in Sec. III. B and anomalously enhanced light emission during the beam injection at 80 mA evidently indicate the ignition of the beam plasma discharge in space. The light excitation near the rocket wall observed by photometer B was detected only for the 80-mA beam. This implies that the energetic electrons produced by strong wave-particle interaction existed in a wide region surrounding the rocket.

The reason for the gradual increase of the light intensity in the initial phase of the 6-s long dc injection at 127 s (the first 1–2 s) observed by both photometers A and B is unknown, but the gradual reduction beginning after one-third of the dc injection time to the end of the pulsed injection at 80 mA (4–5%/km for photometer A; 3–4%/km for photometer B) approximately corresponds to the reduction rate of the $N_2$ density with height at the altitude of 150 km (4%/km in the standard ionospheric model). Taking into account the reduction rate of the background $N_2$ density, there is no significant difference of the photon production rate between the dc and pulsing beam injection at 80 mA. By extrapolating the reduction rate of the luminosity with the decrease of the surrounding gas density, the luminosity would reach a level corresponding to direct collisional excitation at an altitude of approximately 200 km. This implies that the BPD would not be excited by the beam injection at 80 mA above 200 km.[14] It is interesting to compare this result with the fact that the beam plasma discharge was not ignited by the beam (5 kV, 300 mA) injected from the more rapidly moving Space Shuttle Spacelab-1 at the altitude of 245 km.[15] In the Spacelab-1 experiment, the beam plasma discharge was ignited only when the beam was injected into a gas plume that was simultaneously ejected from the Orbiter.

### D. Wave Measurements During Beam Emission

Wave measurements during the electron beam emission have been carried out in the three experiments. In the first two experiments, the spectra were rather complex, due to rocket spin modulation. Here, the wave spectra without spin effect in the third experiment are presented. The vlf and hf antennas were located approximately at 1.5m from the electron gun.

*Emission in the High-Frequency Range*

The general features of wave excitation during the beam injection are shown in Figs. 9 (low gain data), 10 (high gain data for dc beam injection), and 11 (high gain data for pulsed beam injection). Waves with a discrete spectrum around 6 and 9.5 MHz result from ground transmitters. The same applies to the broadband background spectrum from 0.6 to 1.6 MHz observed in the high gain mode. At 5 mA, an emission with a sharp spectrum at 0.9 MHz was detected, which corresponds to the plasma frequency of the background ionospheric plasma ($10^4$/cm$^3$). At 10 mA, peaks at 0.9 and 1.3 MHz were detected. At 40 mA, the discrete emissions disappeared, and broadband emission decreasing with frequency appeared in the whistler mode range below 0.5 MHz. At 80 mA, the wave intensity was increased by more than 15 dB on average, and the broadband emission up to the third cyclotron harmonic was detected.

From previous work, the appearance of broadband emission has usually been observed when the beam plasma discharge is ignited. In the large chamber experiment at Johnson Space Center,[16] narrowband emission at or slightly above the electron cyclotron frequency and its harmonics were excited by the beam current just below the critical current for the ignition of BPD, and whistler mode emission with a cutoff at the electron cyclotron frequency and plasma line emission were excited during the BPD. In the WOMBAT experiment by Boswell and Kellogg,[17] a weak line at the electron cyclotron frequency was observed during the pre-BPD phase and two states of BPD were observed. The first state (BPD1) was characterized by a strong line at the plasma frequency (which was usually less than the cyclotron frequency) and weak discharge was observed. In the second state (BPD2), with higher beam current, broadband emission beyond the cyclotron frequency peaked at the plasma frequency was observed accompanying with changes of luminosity and discharge diameter. Although there are differences in the wave spectrum between the two laboratory experiments, which may be attributed to the difference of the beam parameters, the ap-

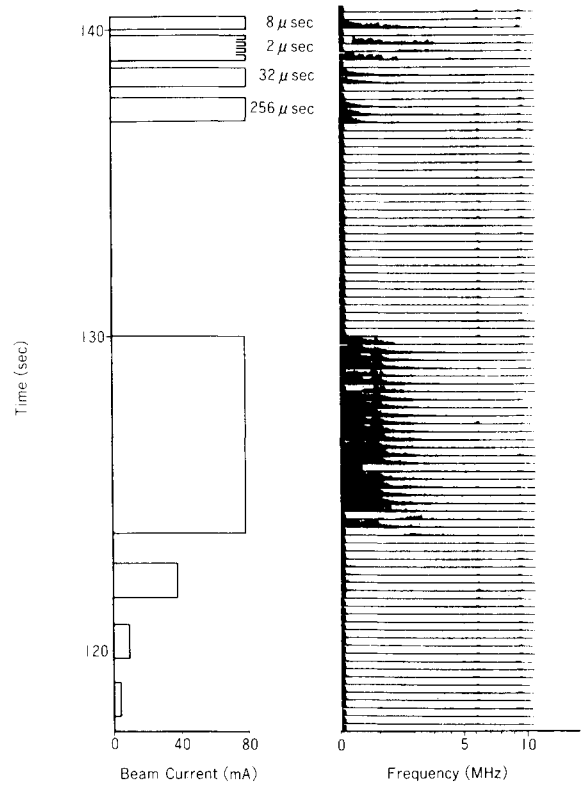


**Fig. 9 Frequency spectrum in hf band (low gain mode).**

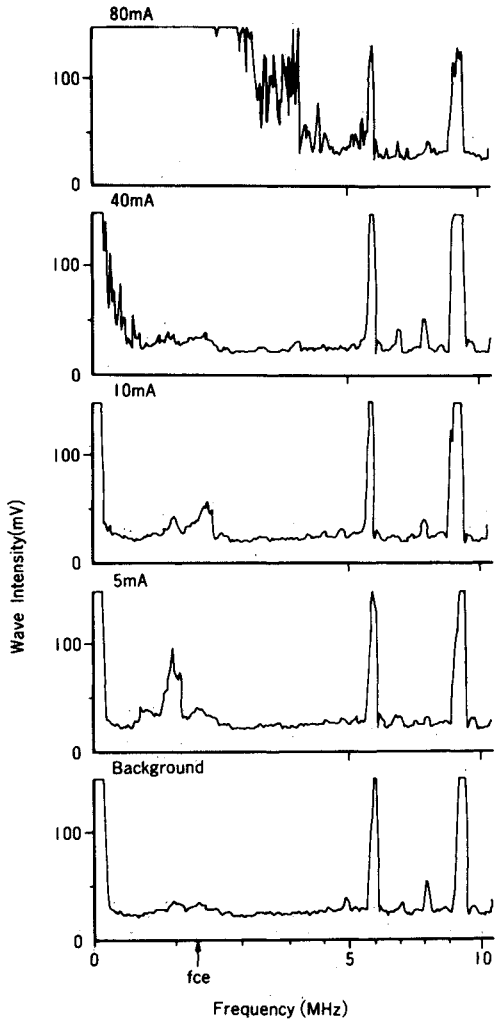


**Fig. 10 Typical frequency spectrum in hf band (high gain mode) during dc beam injection.**

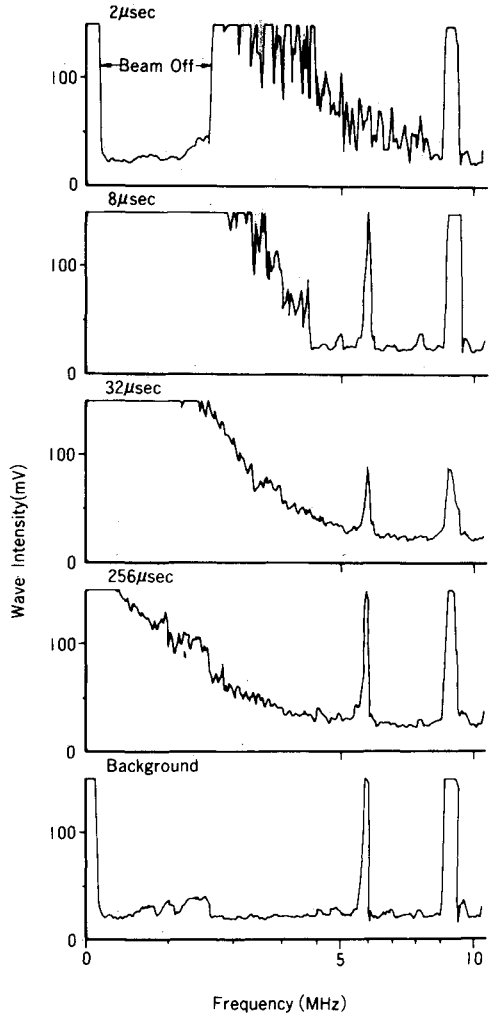


**Fig. 11 Typical frequency spectrum in hf band (high gain mode) during pulsating beam injection.**

pearance of the continuous broadband emission is important evidence for the ignition of the BDP.

In a rocket experiment by Kellogg and Monson,[18] results very similar to the authors', have been obtained. At the smallest beam current (2 keV, 1 mA), they observed little emission in the whistler mode range and a line at the plasma or upper hybrid frequency. In their experiment, by increasing the beam current, the whistler mode emission extended up to the cyclotron frequency, and finally formed an almost featureless continuum extending far beyond the electron cyclotron frequency.

In the pulsating mode of operation, wave emission at the fundamental and harmonics of the modulation frequency was detected for the beam of 2-$\mu$s pulsing (modulation frequency, 250 kHz) in Fig. 9. AT 8, 32- and 256-$\mu$s pulsing (modulation frequencies of 62.5, 15.6, and 1.95 kHz), the discrete spectra for the fundamental and harmonics of the modulation frequency were not detected due to the larger bandwidth of the receiver (100 kHz). Figure 11 shows the typical wave spectra in high gain mode. Comparing to the dc injection at the same beam current (80 mA), the wave intensity is generally smaller, except for 2- and 8-$\mu$s pulsing. However, considering the duty ratio of the gun operation (50%), the wave intensity in the pulsating injection is the same or larger than that in the dc mode. The wave intensity is evidently larger than that in the dc injection at 40 mA, which is equivalent in regard to average power (average current). The type of wave spectrum in the pulsating injection is broadband, as in the dc injection at 80 mA.

The intensity of the radio wave from the ground stations at 6 and 9.5 MHz was remarkably reduced during the beam emission at 80 mA, as is shown in Fig. 9. The wave at 6 MHz sometimes almost disappeared. This means that the electromagnetic wave from the ground stations was shielded by the plasma cloud produced by the beam plasma discharge. The shielding of the 6-MHz electromagnetic wave corresponds to the plasma density $8 \times 10^5/\text{cm}^3$ with a scale of one wavelength (50 m), or to larger density with smaller scale. The fluctuation of the radio wave intensity indicates the fluctuation of the plasma density or the cloud scale generated by the beam emission.

*Emission in the Low-Frequency Range*

During the dc beam injection, a broadband emission decreasing with frequency in average was obtained, as shown in Fig. 12. No clear discrete spectrum was detected. The broadband emission in the vlf range has commonly been observed in the past electron beam experiments by sounding rockets[19,20] and in the SEPAC Space Shuttle Spacelab-1 experiment.[21] However, the wave mode and mechanism of generation have not been clarified as yet. Since the same type of spectrum has also been obtained in a ground laboratory experiment,[22] the mode is not whistler type with long wavelength. It is possibly related to the discharge noise caused by the beam injection,[20] to decay instabilities of hf waves,[23] or to drift wave instabilities.[24] In the pulsed injection, the wave level was comparatively lower than in the dc mode, which can be explained by the duty ratio of beam emission (50%). The

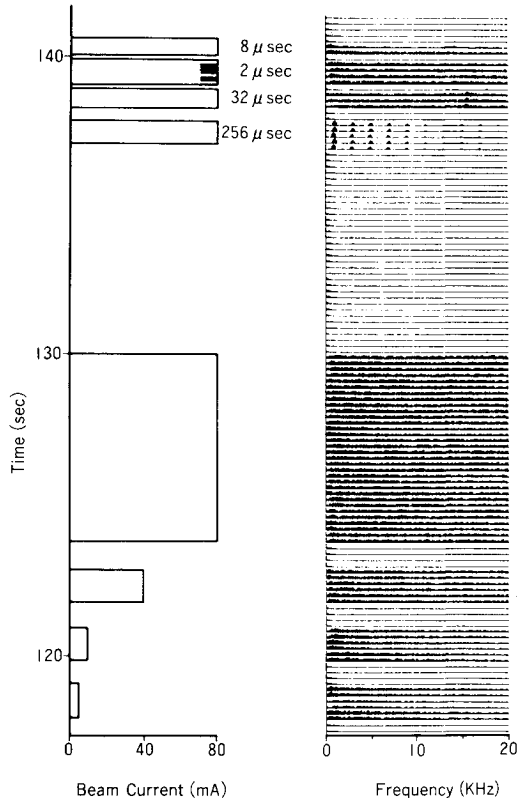


**Fig. 12 Frequency spectrum in vlf band (0.4–20 kHz).**

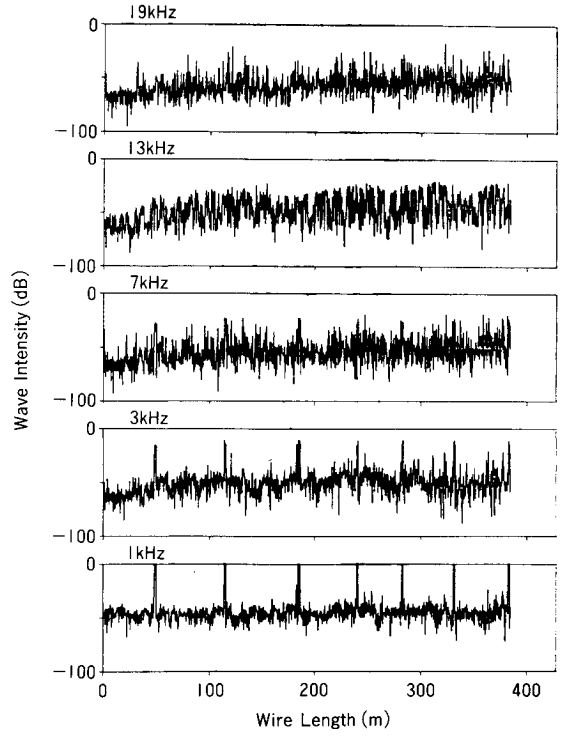


**Fig. 14 Wave intensity at each frequency (vlf band) plotted against the wire length.**

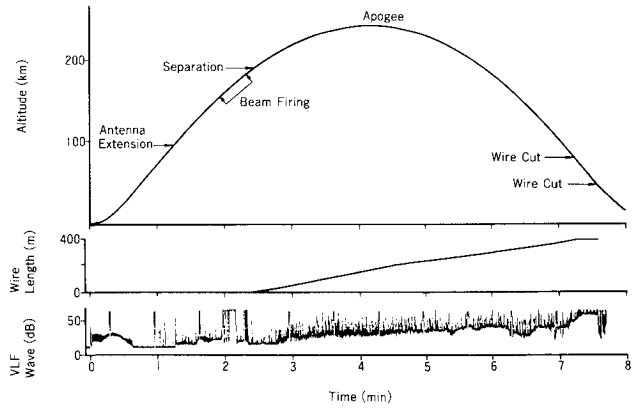


**Fig. 13 Time variation of integrated wave intensity up to 30 kHz.**

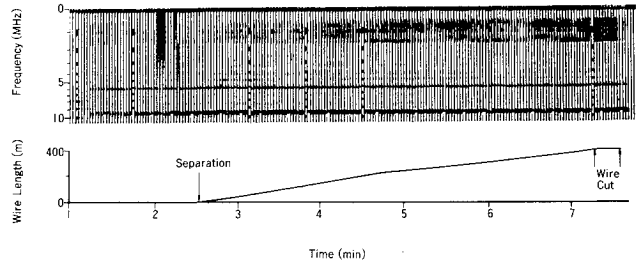


**Fig. 15 Time variation of hf spectrum during flight.**

modulation frequencies at 1.95 kHz (256-$\mu$s pulsing) and 15.6 kHz (32-$\mu$s pulsing) were within the measurable range of the receiver. During 1.95-kHz modulation, the receiver was in the calibration mode, but at 15.6-kHz modulation, a discrete emission at 15.6 kHz was detected. Since the antenna was located near the beam path, little can be said as to whether the emission could propagate away or not. According to the rocket experiment by Holzworth and Koons,[25] vlf emission from a modulated electron beam at 3 kHz could be detected at 1.4-km separation although the beam was possibly disturbed by the beam plasma discharge.

### E. Wave Enhancement When the Tether Wire is Extended

In the third experiment, the tether wire was extended up to 418 m. The wave intensity observed both by hf and vlf receivers was remarkably changed with the wire extension.

*Enhancement of vlf Emission*

Figure 13 shows the variation of the integrated wave intensity from 0.4 to 30 kHz with time. The integrated intensity increased after the start of the wire deployment. It abruptly decreased at 454 s, when the wire was cut near the daughter payload. No remarkable change was detected when the tether wire was cut at the mother payload at 436 s. This indicates that the tether wire acted as a vlf antenna. Note that the tether wire was not connected to the receiver input, but to the ground of the daughter payload only. The background vlf noise is presumed almost constant near the apogee (altitude from 200 to 218 km). In this region (ascending and descending), the wire was deployed from 60 to 270 m (6.5 dB in length) during 135 s. During that period, the detected wave intensity increased by about 8 dB. This means that the antenna impedance of the tether wire decreased almost in inverse proportion to the wire length. Figure 14 shows the changes of the wave intensity at 1, 3, 7, 13, and 19 kHz plotted against the wire length. The increase of the wave intensity with the wire length near the apogee (wire length 60–270 m) is seen similarly at each frequency range. The spiky signals shown below 7 kHz correspond to instrument calibration.

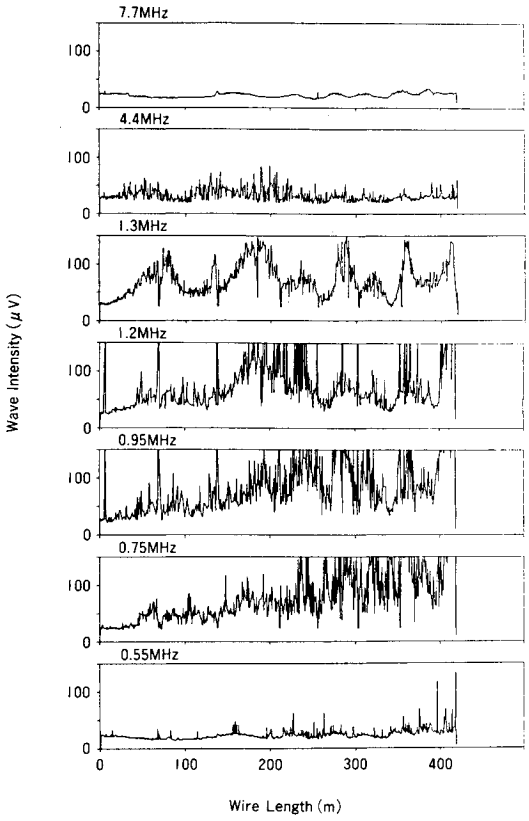


**Fig. 16 Wave intensity at each frequency (hf band) plotted against the wire length.**

*Enhancement of hf Emission*

Waves in the hf range at 0.6–1.6, 5, 6, and 9.5 MHz were detected at almost all flight times after the antenna extension even after the re-entry. Their source must be located on the ground. The wave intensity of 0.6–1.6 MHz (wavelength 500–188 m) was remarkably changed with the deployment of the tether wire, as shown in Fig. 15. The measured wave intensity decreased abruptly at 454 s, when the tether wire was cut near the daughter payload. This means that the wire acted as a high-frequency antenna in this band, although it was not connected to the hf wave receiver. The variation of the wave intensity at each frequency band is shown in Fig. 16. At low frequencies, less than 0.75 MHz (wavelength longer than 400 m), the average intensity increased monotonically with the wire length. At 0.95 MHz (wavelength 315 m), the intensity peaked at around 300 m. At 1.2 MHz (wavelength 250 m), the intensity was maximum around 200 m. At 1.3 MHz (wavelength 230 m), the intensity was strongly modulated by the spin motion of the daughter payload. Above 1.6 MHz (wavelength less than 190 m), the intensity did not change remarkably. The antenna impedance of the tether wire decreased with the wire length for the radio waves below 1.6 MHz, but did not clearly change above 1.6 MHz. This cannot be explained by the theory of simple dipole antennas. It will be investigated elsewhere related to the theory of antenna impedance in space plasma.

## IV. Conclusion

The series of tethered rocket experiments has provided reproducible data of the vehicle charging by the electron beam emission. The potential of the vehicle that emits a dc electron beam up to 80 mA at an altitude of from 150 to 200 km in the ionosphere is usually less than 10 V. This cannot be explained without considering plasma production by the beam plasma discharge. The evidence for the ignition of the beam plasma discharge during 80-mA injection at around 150 km has been clearly obtained by light and wave measurements. The light emission at 3914 Å was greatly enhanced, and continuous broadband radio emission extending beyond the cyclotron frequency was detected. These features coincide with the experimental results on the beam plasma discharge in the ground laboratory experiments.

The dynamics of tether wire and the effect of the wire deployment on the wave measurements have also been studied. It has been found that the tether wire acted as a wave antenna, and the antenna impedance decreased with the tether length in both the very low-frequency and high-frequency bands up to 1.6 MHz. This suggests that a tether wire system can act as an effective wave transmitter with low impedance in future experiments when radio frequency is applied to the wire in active experiments.

## Acknowledgment

A portion of this work was funded through NASA Grant NAGW-235 at Stanford University.

## References

[1]Banks, P.M., Williamson, P.R., and Oyama, K.I., "Shuttle Orbiter Tethered Subsatellite for Exploring and Tapping Space Plasmas," *Astronautics & Aeronautics,* Feb. 1981, pp. 31–33.

[2]Winckler, J.R., Steffen, J.E., Malcolm, P.R., Erickson, K.N., Abe, Y., and Swanson, R.L., "Ion Resonances and ELF Wave Production by an Electron Beam Injected into the Ionosphere: Echo 6," *Journal of Geophysical Research,* Vol. 89, 1984, pp. 7565–7571.

[3]Möbius, M., Haerendel, G., Brenning, N., and Axnäs, I., "Zenon Release Experiment from Shuttle on Alfvén's Critical Ionization Velocity Using the Tethered Satellite System," Technical Proposal for NASA/PSN, July 1984.

[4]Colombo, G., Gaposchkin, E.M., Grossi, M.D., and Weiffenbach, G.C.,"Shuttle Borne Skyhook; A New Tool for Low Orbital-Altitude Research," Proposal by Smithsonian Institute Astrophysical Observatory, Sept. 1974.

[5]Rupp, C.C., "A Tether Tension Control Law for Tethered Subsatellites Deployed Along Local Vertical," NASA TMX-64963, Sept. 1975.

[6]Baker, W.P., et al., "Tethered Subsatellite Study," NASA TMX-73314, April 1976.

[7]Williamson, P.R. et al., "Measurements of Vehicle Potential Using a Mother-Daughter Tethered Rocket," *Artificial Particle Beams in Space Plasma Studies,* edited by B. Grandal, Plenum, New York, 1982, pp. 645–653.

[8]Yokota, T., Sasaki, S., Kawashima, N., Oyama, K., and Nakai, Y., "Observation of Daughter Payload and Tether Wire by CCD Camera Onboard S-520-2 Rocket," ISAS RN 209, 1983.

[9]Kawashima, N., Sasaki, S., Oyama, K., Akai, K., and Nakai, Y., "Floating Potential and Return Current Measurements in a Rocket-Borne Electron Beam Experiment," *Geophysical Research Letters,* Vol. 9, 1982, pp. 1061–1063.

[10]Beard, D.B. and Johnson, F.S., "Ionospheric Limitations on Attainable Satellite Potential," *Journal of Geophysical Research,* Vol. 66, 1961, pp. 4113–4122.

[11]Parker, L.W. and Murphy, B.L., "Potential Buildup on an Electron-Emitting Ionospheric Satellite," *Journal of Geophysical Research,* Vol. 72, 1967, pp. 1631–1636.

[12]Linson, L.M., "Current-Voltage Characteristics of an Electron-Emitting Satellite in the Ionosphere," *Journal of Geophysical Research,* Vol. 74, 1969, pp. 2368–2375.

[13]Hallinan, T.J., Leinbach, H., and Bernstein, W., "Visible Signatures of the Multi-Step Transition to a Beam-Plasma-Discharge," *Artificial Particle Beams in Space Plasma Studies,* edited by B. Grandal, Plenum, New York, 1982, pp. 339–349.

[14]Linson, L.M., "Charge Neutralization as Studied Experimentally and Theoretically," *Artificial Particle Beams in Space Plasma Studies,* edited by B. Grandal, Plenum, New York, 1982, pp. 573–595.

[15]Sasaki, S. et al., "Ignition of Beam Plasma Discharge in the Electron Beam Experiment in Space," *Geophysical Research Letters,* Vol. 12, 1985, pp. 647–650.

[16]Bernstein, W., Leinbach, H., Kellogg, P.J., Monson, S.J., and Hallinan, T., "Further Laboratory Measurements of the Beam-Plasma Discharge," *Journal of Geophysical Research,* Vol. 84, 1979, pp. 7271–7278.

[17]Boswell, R.W. and Kellogg, P.J., "Characteristics of Two Types Beam Plasma Discharge in a Laboratory Experiment," *Geophysical Research Letters,* Vol. 10, 1983, pp. 565-568.

[18]Kellogg, P.J. and Monson, S.J., "A Second Kind of BPD—Rocket and Laboratory Results," *Active Experiments in Space,* Proceedings of an International Symposium held in Alpbach, Austria, 1983, pp. 157-159.

[19]Cartwright, D.G. and Kellogg, P.J., "Observations of Radiation from an Electron Beam Artificially Injected into the Ionosphere," *Journal of Geophysical Research,* Vol. 79, 1974, pp. 1439-1457.

[20]Grandal, B., Holttet, J.A., Troim, J., Maehlum, B., and Pran, B., "Polar 5: Observations of Waves Artificially Stimulated by an Electron Beam Inside a Region with Auroral Precipitation," Norwegian Defence Research Establishment, Kjeller, Norway, FFI/RAPPORT-80/7004, March 1980.

[21]Akai, K., "Electron Beam-Plasma Interaction Experiment in Space," ISAS RN 285, 1985.

[22]Sasaki, S., Hori, T., Nomoto, K., Uehara, K., and Obayashi, T., MTV/SODA-QL Joint Report on the Third NASDA-SEPAC Test (summary), ISAS RN 187, July 1982.

[23]Llobet, X., Bernstein, W., and Konradi, A., "The Spatial Evolution of Energetic Electrons and Plasma Waves During the Steady State Beam Plasma Discharge," *Journal of Geophysical Research,* Vol. 90, 1985, pp. 5187-5196.

[24]Neubert, et al., "Waves Generated During Electron Beam Emissions from the Space Shuttle," *Journal of Geophysical Research,* Vol. 91, 1986 pp. 1132-1329.

[25]Holzworth, R.H., and Koons, H.C., "VLF Emissions from a Modulated Electron Beam in the Auroral Ionosphere, " *Journal of Geophysical Research,* Vol. 86, 1981, pp. 853-857.